J Wood Sci (2007) 53:100–107
DOI 10.1007/s10086-006-0823-2

ORIGINAL ARTICLE

Ying Gao · Masamitsu Ohta

Deformation analysis of timber-framed panel dome structure I: simulation of a dome model connected by elastic springs

Received: April 7, 2006 / Accepted: June 12, 2006 / Published online: October 8, 2006

Abstract This study develops an analytical method that enables the simulation of the deformation of timber-framed plywood panel dome structures, of which strength is largely governed by the rigidity of joints. A hybrid truss structure model was employed to analyze this structure. In this model, we aimed to incorporate the mechanical properties of bolted and nailed joints, which were employed to build the structures, although the present investigation focused on the deformation characteristics of a dome in which the panel elements were connected mutually by elastic springs. The results of the theoretical analysis are compared with those obtained by experiments. The simulated results were found to be in good agreement with the results of the experiments under similar loading conditions.

Key words Timber-framed panel dome structure · Numerical simulation · Hybrid truss structure

Introduction

Timber-framed panel dome structure

Wooden geodesic domes consist of intersecting timber ribs forming a triangulated truss structure.[1] The majority of modern domes are built as truss structures; in this case, panels covering the dome do not serve as the primary structural members. Another kind of dome structure consists of paneled triangular frames that are connected by bolts. Timber-framed panel dome (TPD), the structure studied here, is one of such wooden geodesic domes. In the case of TPD, frames made from 2 × 4s (50 × 100-mm cross-section dimensions) are bolted together and fitted with plywood with nails (Fig. 1). Therefore, the strength of the structure depends mainly on the joint part of every neighboring triangular framed panel. However, TPD can often be analyzed by being approximated as a three-dimensional (3D) truss structure. Although the neighboring frame panels are likely to separate from each other, it is impossible to simulate the deformation process of the joint parts by simple 3D truss analysis.

The main focus of this study was to develop a method to simulate joint deformation in TPD structures. The simulation result was compared with that of the simple truss approximation. Joint parts consisted of bolts and nails and were analyzed as components of an elastoplastic structure. As a preliminary study, the joint parts were treated here as elastic springs. We also made a corresponding dome model with joint parts connected by elastic cords.

Proper method for simulating the TPD

Stress analysis of wooden dome structures has been carried out mainly using the classical finite element method (FEM).[2] As a preliminary study, the TPD structural analysis was carried out by FEM as a simple 3D truss structure consisting of 105 truss elements and 46 nodes. It was later determined that the 3D truss structure program could not be applied to the TPD structure after comparing the output with the experimental result.

Next, the applied element method (AEM)[4] was used. The AEM is an effective method for simulating highly nonlinear behavior, i.e., crack initiation, crack propagation, separation of structural elements, rigid body motion of failed elements, and collapse process of the structure. In our case, every two neighboring triangle elements needed to be connected by distributed springs in normal and tangential directions. The coordinate treatment was found to become too complicated in the three-dimensional case.

Another approach based on FEM was proposed to numerically analyze the TPD structure. Here, we call it a "hybrid truss structure." In the hybrid truss structure

Y. Gao (✉) · M. Ohta
Graduate School of Agricultural and Life Science, The University of Tokyo, Tokyo 113-8657, Japan
Tel. +81-3-5841-5249; Fax +81-3-5684-0299
e-mail: aa37403@mail.ecc.u-tokyo.ac.jp

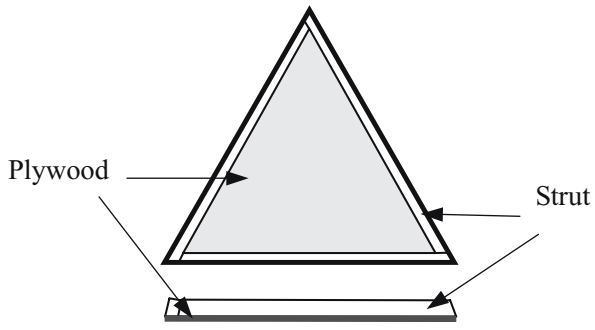

Fig. 1. Paneled triangle frame

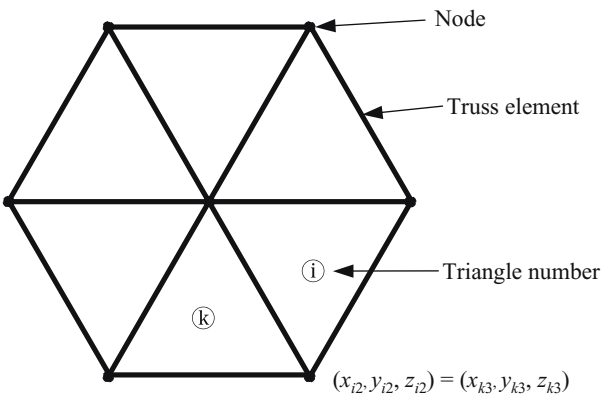

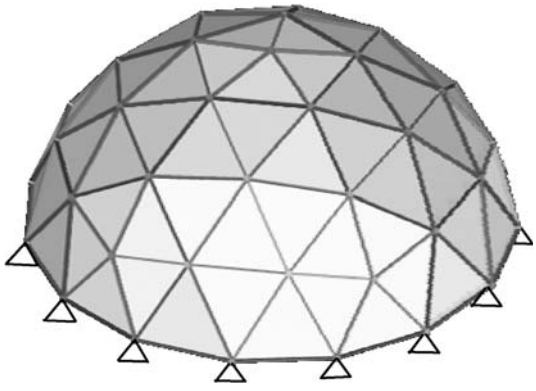

Fig. 2. Timber-framed panel dome (TPD) used in this study[3]

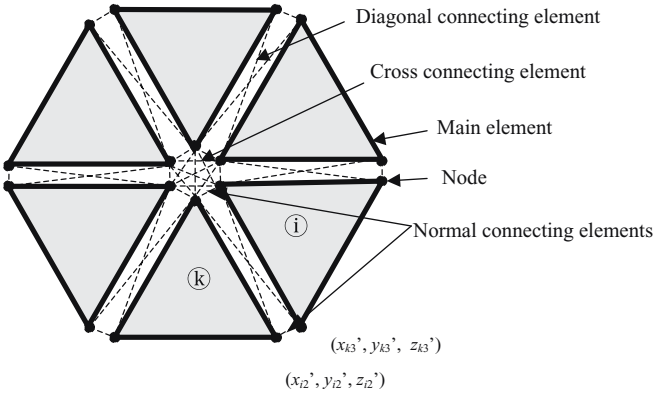

Fig. 3. Hexagonal unit of simple truss structure (*upper*) and hybrid truss structure (*lower*)

model, the TPD structure was assumed to be a complicated 3D truss structure.

Theories

Transformation from simple truss to hybrid truss

A TPD (Fig. 2) was selected to study joint deformation behavior. In our hybrid truss structure, each triangular element is represented by high modulus bar elements and these triangular trusses are separated from each other. The semirigid triangular elements are then connected by many weak modulus bar elements (Fig. 3). In the first step, a pretreatment program was made to convert the original simple truss dome to a separated triangular structure by magnifying the hemisphere dome by the ratio of $1 + \alpha$ along the radial direction, which passes though the center of gravity within each dome triangle (Fig. 4). We intended to give the characteristics of connecting properties to the clearance between triangular elements. The origin of the coordinate system was defined as the center of hemisphere dome.

The coordinate of the new model is calculated as follows:

$$\begin{aligned} x'_{ij} &= x_{ij} + \Delta x_i, \\ y'_{ij} &= y_{ij} + \Delta y_i, \\ z'_{ij} &= z_{ij} + \Delta z_i, \end{aligned} \tag{1}$$

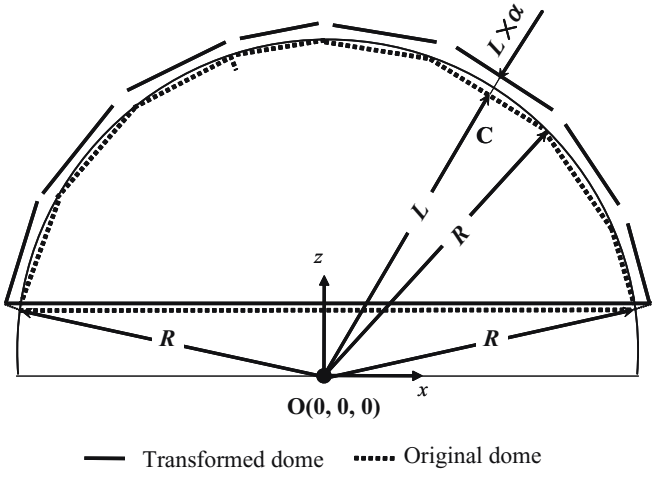

Fig. 4. Transformation from the simple truss to the hybrid truss. *O*, center of gravity in the sphere from which dome derived; *C*, center of gravity in isosceles triangular frames; *R*, radius of sphere from which dome derived; *L*, distance from point O to point C; α, amplification ratio

$$\begin{aligned} \Delta x_i &= \alpha x_{ic} = \frac{\alpha}{3}\sum_{j=1}^{3} x_{ij}, \\ \Delta y_i &= \alpha y_{ic} = \frac{\alpha}{3}\sum_{j=1}^{3} y_{ij}, \\ \Delta z_i &= \alpha z_{ic} = \frac{\alpha}{3}\sum_{j=1}^{3} z_{ij}, \end{aligned} \tag{2}$$

where x_{ij}, y_{ij}, and z_{ij} represent the original coordinates of point j of triangle i, respectively, and x'_{ij}, y'_{ij}, and z'_{ij} represent the triangular unit's new coordinates. Δx_i, Δy_i, and Δz_i are the increment of x-, y-, and z-coordinates, which are equal to α-times of the coordinate of the center of gravity for triangle i, x_{ic}, y_{ic}, and z_{ic}. The value of 0.06 was employed for α, considering the thickness of the neighboring beams.

Morphology of hybrid truss structure

Based on the method described above, a new dome structure (Fig. 5) was obtained. Triangular elements were jointed by three kinds of springs: normal springs, diagonal springs, and cross springs (Fig. 3). The newly obtained hybrid truss structure may be modeled as a 3D truss structure, but the modeled results showed disagreement with the experimental structure (Fig. 6). Rotational springs were later added to the truss structure and it was retested. Comparison of a number of simple truss structures and the newly obtained hybrid truss structures are shown in Table 1.

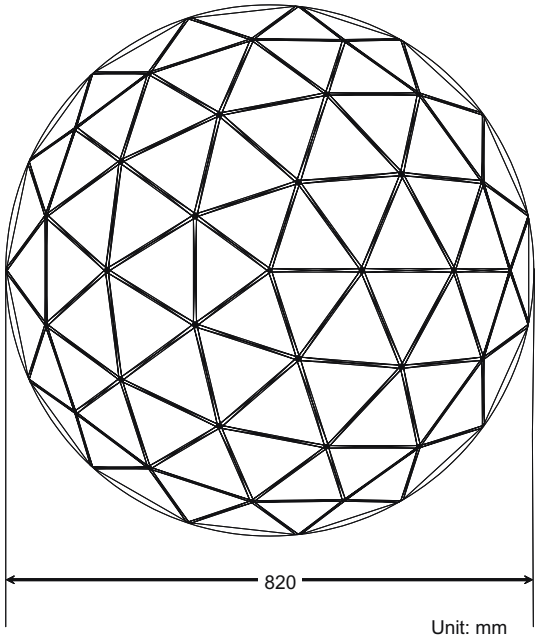

Fig. 5. TPD structure hybrid truss (top view)

Derivation of stiffness matrix

The stiffness matrix was derived by the following processes:[5] the stiffness equation can be represented as:

$$\{F\} = [K]\{\delta\}, \tag{3}$$

where $\{F\}$ represents the vector of forces acting on the nodes, $[K]$ is the stiffness matrix, and $\{\delta\}$ is the displacement vector.

As mentioned above, the dome structure was transformed to main truss elements and connecting elements. The main elements were defined as truss elements, with high Young's modulus, and the spring elements with small elastic coefficients. A truss element can only transmit forces in an axis direction, and then the stiffness matrix of it in a local coordinate system can be represented as:

$$\left[K_1^e\right] = \frac{AE}{L}\begin{bmatrix} 1 & 0 & 0 & -1 & 0 & 0 \\ 0 & 0 & 0 & 0 & 0 & 0 \\ 0 & 0 & 0 & 0 & 0 & 0 \\ -1 & 0 & 0 & 1 & 0 & 0 \\ 0 & 0 & 0 & 0 & 0 & 0 \\ 0 & 0 & 0 & 0 & 0 & 0 \end{bmatrix}, \tag{4}$$

where A is the cross-sectional area of the element, E is the Young's modulus, and L is the length of the element.

The coordinate transfer matrix was then employed to convert the local coordinate stiffness matrix into the global one:

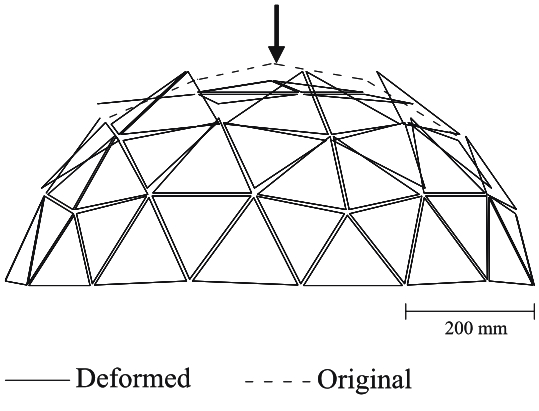

Fig. 6. Calculated deformation of TPD structure without rotational springs. Displacement of the top apex is 26.6 mm downward

Table 1. Comparison of elements' members between simple truss system and hybrid truss system

Type	Node number	Triangle number	Main truss	Connecting truss			Rotation spring
				Normal	Diagonal	Cross	
Simple truss	46	75	105	–	–	–	–
Hybrid truss	225	75	225	210	210	270	1830

For definitions of connecting truss, see Fig. 3

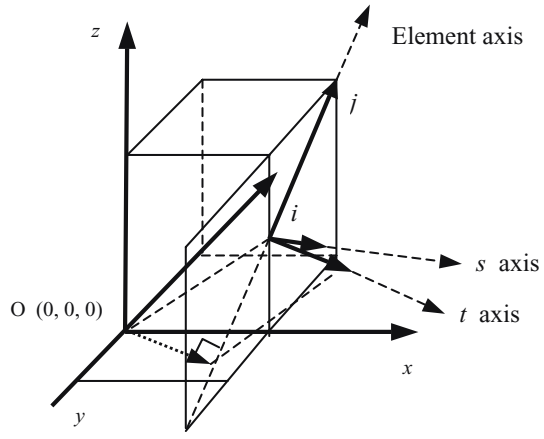

Fig. 7. Three directions of a truss element: element axis, *t* axis, and *s* axis (*i* and *j* are point number of an element)

$$[K_1] = [T_1]^T [K_1^e][T_1], \tag{5}$$

$$T_1 = \begin{bmatrix} l_1 & m_1 & n_1 & 0 & 0 & 0 \\ 0 & 0 & 0 & 0 & 0 & 0 \\ 0 & 0 & 0 & 0 & 0 & 0 \\ 0 & 0 & 0 & l_1 & m_1 & n_1 \\ 0 & 0 & 0 & 0 & 0 & 0 \\ 0 & 0 & 0 & 0 & 0 & 0 \end{bmatrix}, \tag{6}$$

where l_1, m_1, and, n_1 are the direction cosines of axis direction, which will be explained later.

The rotation spring elements require two stiffness resistances around the rotational axis. One is from the center of sphere perpendicular to the axis direction of the element, which we call *t* axis. The other is the normal to the plane composed by the element axis and *t* axis, and we refer to it as the *s* axis (see Fig. 7).

The stiffness matrix of rotation spring around the *t* axis is:

$$[K_2] = [T_2]^T [K_2^e][T_2], \tag{7}$$

where

$$[K_2^e] = \frac{k_{s1}}{L^2} \begin{bmatrix} 0 & 0 & 0 & 0 & 0 & 0 \\ 1 & 0 & 0 & -1 & 0 & 0 \\ 0 & 0 & 0 & 0 & 0 & 0 \\ 0 & 0 & 0 & 0 & 0 & 0 \\ -1 & 0 & 0 & 1 & 0 & 0 \\ 0 & 0 & 0 & 0 & 0 & 0 \end{bmatrix}, \tag{8}$$

where k_{s1} is the elastic coefficient of the rotation spring around the *t* axis and the corresponding coordinate transform matrix T_2 is:

$$T_2 = \begin{bmatrix} 0 & 0 & 0 & 0 & 0 & 0 \\ l_2 & m_2 & n_2 & 0 & 0 & 0 \\ 0 & 0 & 0 & 0 & 0 & 0 \\ 0 & 0 & 0 & 0 & 0 & 0 \\ 0 & 0 & 0 & l_2 & m_2 & n_2 \\ 0 & 0 & 0 & 0 & 0 & 0 \end{bmatrix}, \tag{9}$$

Analogously, the stiffness matrix around the *s* axis is:

$$[K_3] = [T_3]^T [K_3^e][T_3], \tag{10}$$

where

$$[K_3^e] = \frac{k_{s2}}{L^2} \begin{bmatrix} 0 & 0 & 0 & 0 & 0 & 0 \\ 0 & 0 & 0 & 0 & 0 & 0 \\ 1 & 0 & 0 & -1 & 0 & 0 \\ 0 & 0 & 0 & 0 & 0 & 0 \\ 0 & 0 & 0 & 0 & 0 & 0 \\ -1 & 0 & 0 & 0 & 0 & 0 \end{bmatrix}, \tag{11}$$

where k_{s2} is the elastic coefficient of rotation spring around the *s* axis and the corresponding coordinate transform matrix T_3 is:

$$T_3 = \begin{bmatrix} 0 & 0 & 0 & 0 & 0 & 0 \\ 0 & 0 & 0 & 0 & 0 & 0 \\ l_3 & m_3 & n_3 & 0 & 0 & 0 \\ 0 & 0 & 0 & 0 & 0 & 0 \\ 0 & 0 & 0 & 0 & 0 & 0 \\ 0 & 0 & 0 & l_3 & m_3 & n_3 \end{bmatrix}. \tag{12}$$

Consequently, the stiffness matrix is:

$$[K] = [K_1] + [K_2] + [K_3]. \tag{13}$$

Derivation of direction cosine

The direction cosines l_i, m_i, and n_i can be calculated as follows. Assuming the start point of the element is *i* (x_i, y_i, z_i) and the end point is *j* (x_j, y_j, z_j), then direction cosines of the axial direction are:

$$\begin{aligned} l_1 &= \frac{x_j - x_i}{L}, \\ m_1 &= \frac{y_j - y_i}{L}, \\ n_1 &= \frac{z_j - z_i}{L}, \end{aligned} \tag{14}$$

where $L = \sqrt{(x_j - x_i)^2 + (y_j - y_i)^2 + (z_j - z_i)^2}$ is the length of the element.

The vector from point *i* to the center of sphere *k* (0,0,0) can be written as:

$$\overrightarrow{ik} = l_0\bar{x} + m_0\bar{y} + n_0\bar{z}$$
$$l_0 = \frac{-x_i}{B},$$
$$m_0 = \frac{-y_i}{B}, \quad (15)$$
$$n_0 = \frac{-z_i}{B},$$

and $B = \sqrt{x_i^2 + y_i^2 + z_i^2}$.

Direction cosines of the s axis are:

$$l_3 = \frac{m_1 n_0 - n_1 m_0}{D},$$
$$m_3 = \frac{n_1 l_0 - l_1 n_0}{D}, \quad (16)$$
$$n_3 = \frac{l_1 m_0 - m_1 l_0}{D},$$

where $D = \sqrt{(m_1 n_0 - n_1 m_0)^2 + (n_1 l_0 - l_1 n_0)^2 + (l_1 m_0 - m_1 l_0)^2}$.

Direction cosines of the *t* axis are:

$$l_2 = m_3 n_1 - n_3 m_1,$$
$$m_2 = n_3 l_1 - l_3 n_1, \quad (17)$$
$$n_2 = l_3 m_1 - m_3 l_1.$$

Deformation compatibility of triangle panels

Although the dome has been transformed to the separated triangle system, considering that the triangular panels cannot be overlapped in the real buildings even under compression stress, the distance between every two neighboring triangles should be kept almost constant. The modulus of the connecting elements in our research varied with the direction of the acting forces. Once a connection spring received a compression force, its Young's modulus increased to that of main elements, while it was unchanged in the tension cases.

An iteration method was employed to solve Eq. 3 and the solution was obtained as a converged result by satisfying:

$$\mathrm{Max}\left(\left|\frac{dl_i' - dl_i}{dl_i}\right|\right) \le 0.001 \quad (18)$$

where dl_i' is the deformation of element *i* at a previous loop, and dl_i is the deformation of element *i* in the current loop.

Simulations

Simulated model structures

The TPD in this study is a 3 frequency (3v) icosahedron dome,[6] which was invented by Buckminster Fuller. The 3v domes are made up of two basic shapes of isosceles triangles arranged in groups. There are seven and a half groups of six panels each, called hexagonal groups, and six groups of five panels each, called pentagonal groups. The stiffness values are summarized in Table 2, where *A* is the area of the elements, and *E* is the Young's modulus of the wood beam in the main truss. Young's modulus *E* of the connecting truss was calibrated by the real model experiment, and the elastic coefficient values of rotation springs were also calibrated. The effect of element mass was neglected.

Materials and methods

Spruce was used for the triangular frame, and the triangle panels were made of plywood. The sizes of the panels are shown in Fig. 8. The thickness of the plywood was 2.5 mm. Wood panels were adhered to the triangular timber frame. The sides of the triangular frame were drilled and were fastened to each other by elastic bands with a diameter of 1.5 mm.

The experiment was designed to measure the deformation of the whole dome structure (Fig. 9). The dome model was laid on a plain board that was fixed on a rotary turntable. The base of the dome was secured by a fixture. Load was added to specific nodes in vertical and horizontal directions separately. Deformation of the whole dome was scanned and digitized by a 3D digital scanner (VIVID 910, Konica Minolta). The dome model was scanned from several different perspectives, and then merged into a

Table 2. Constants used for the calculation

Coefficient	Main truss	Connecting truss			Rotation spring
		Normal	Diagonal	Cross	
$A \cdot E$ (N)	342 900	0.05	0.05	0.05	–
K_{s1} (N·mm)	–	–	–		0.5
K_{s2} (N·mm)	–	–	–	–	0.5

A, Area of elements' cross section (unit: mm^2); *E*, Young's modulus of elements (unit: N/mm^2); K_{s1}, elastic coefficient of rotation spring around *t* axis; K_{s2}, elastic coefficient of rotation spring around *s* axis

single mesh. The obtained pictures were integrated and analyzed by the software package Rapidform 2004 (Inus Technology).

Results and discussion

Loads were added to the top nodes of the simple truss structure and a hybrid truss structure until the top nodes bowed to the same height of the other nodes of the top pentagon. The deformation aspect of the simple truss calculation is shown in Fig. 10a, b. With the simple truss method, deformation of the whole structure comes from length changes in the trusses (Fig. 11). The results in Fig. 11 indicate that it is not in agreement with reality. Figure 12 shows the experimental result of the TPD. The shape of the triangle did not change at all, while the joint part deformed seriously. Figure 10c shows the original TPD modeled by hybrid truss and the simulated result in Fig. 10d. Details of the deformation of the top pentagon are shown in Fig. 13. The simulated and observed results showed good agreement and therefore validated the use of the hybrid truss method as an effective means of analyzing TPD.

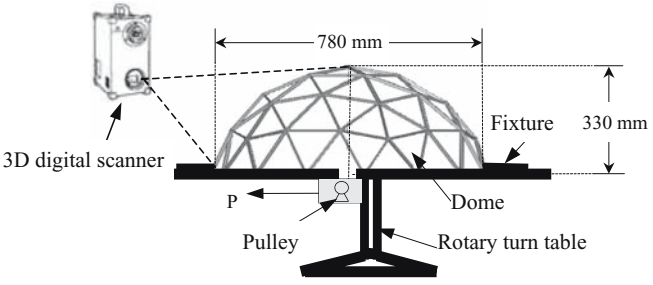

Fig. 9. Dome experimental equipment

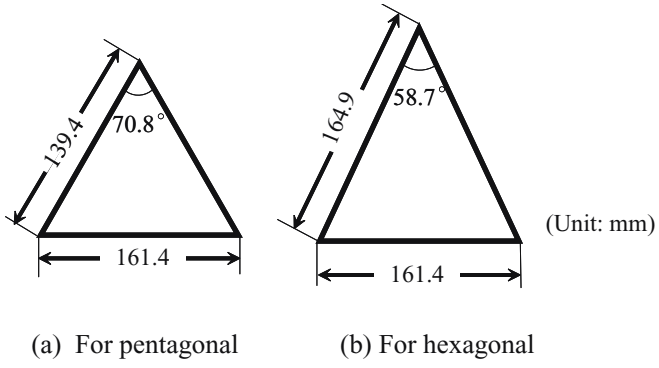

Fig. 8. Isosceles triangles for pentagonal groups and hexagonal groups

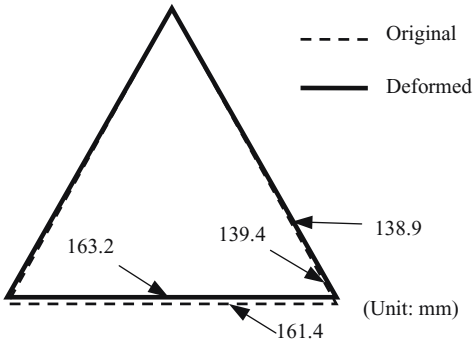

Fig. 11. Deformation aspect of one of the top triangle elements in the simple truss analysis. Significant deformation occurred in the truss unit during the stress testing. This figure shows the specimen in Fig. 10a

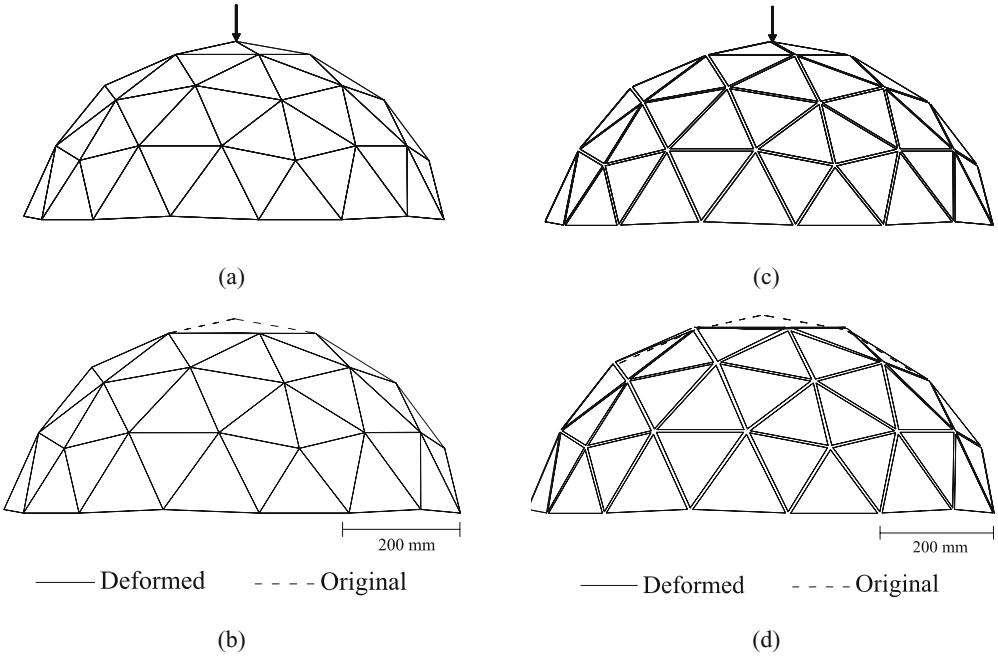

Fig. 10a–d. Comparison of deformation morphology between the simple truss structure (**a**, **b**) and the hybrid truss structure (**c**, **d**) under vertical applied force. Deformation of the top apex in **b** and **d** are both 24.3 mm downward

To make clear the difference of deformation of shape between the simple truss element and the hybrid truss element, calculations were undertaken in which horizontal forces were applied on these two types of domes, respectively. Figure 14 shows the comparison of deformation between these two models. Deformation of the simple truss structure is not obvious from Fig. 14a, b; while the hybrid truss deformation from Fig. 14c to Fig. 14d is clearly visible.

In reality the loading condition described above is difficult to apply. Therefore, the force was added to only a single node at a time. As Fig. 15 shows, four typical nodes were selected to be loaded horizontally and vertically. The results of hybrid truss calculation shown in Table 3 indicate good agreement between calculated and experimental outputs.

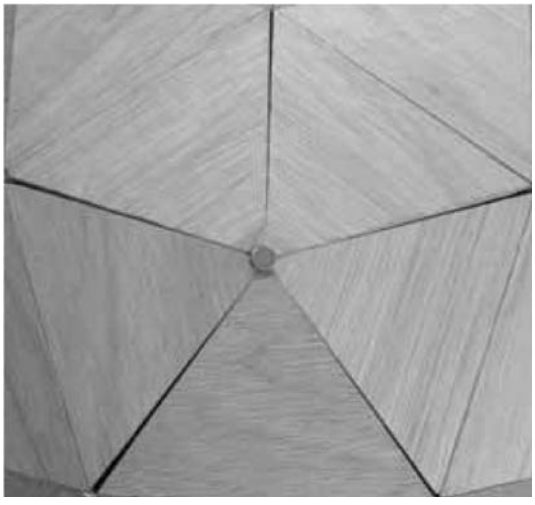

Fig. 12. Deformation of the top pentagon in the experiment, which corresponds to the state shown in Fig. 10d

Conclusions

This article describes the deformation characteristics of a TPD. Experimental observation of a TPD connected by linear elastic springs showed that the elements near the loading point deformed severely under the applied load,

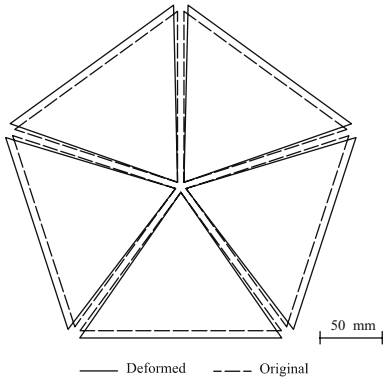

Fig. 13. The deformation of the top pentagonal group obtained from the hybrid truss calculation. The result corresponds to Fig. 12

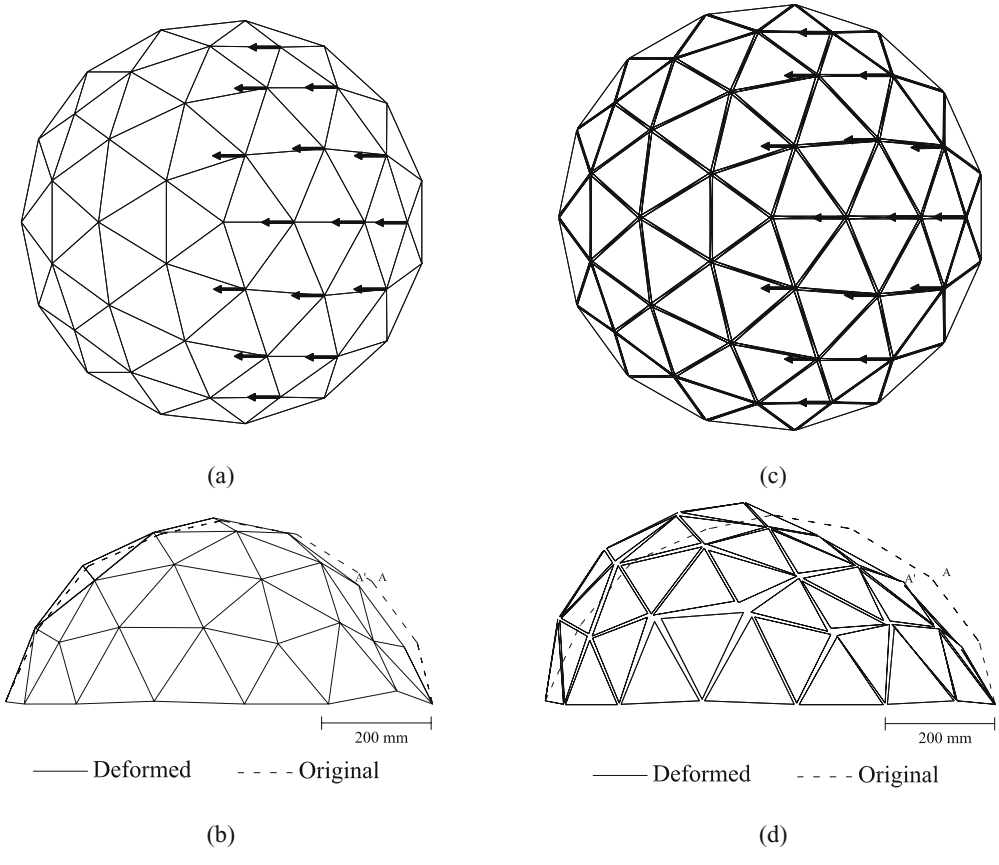

Fig. 14a–d. Comparison of deformation morphology between the simple truss (**a**, **b**) and the hybrid truss (**c**, **d**) under a transverse load. The deformations from A to A′ were 23.4 mm in **b** (total load 4.5 kN), and 53.6 mm in **d** (total load 174 N)

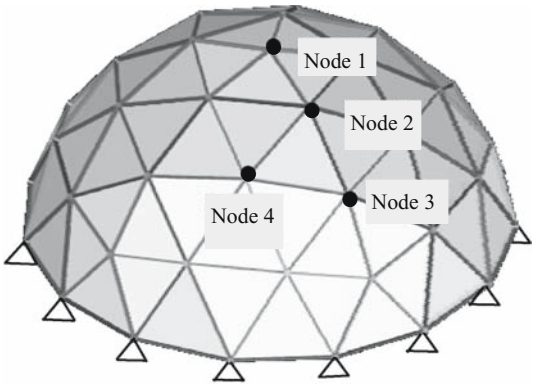

Fig. 15. Loaded nodes in experiment

Table 3. Comparison of deformation between observed and hybrid truss calculation results

Case[a]	Observed (mm/N)	Simulated (mm/N)
Node 1(V)	0.885	0.825
Node 2(V)	0.807	0.670
Node 3(V)	0.432	0.345
Node 4(V)	0.414	0.395
Node 4(H)	0.450	0.465

V, Vertical loading; H, horizontal loading
[a] For nodes 1–4, see Fig. 15

and the weakness of the joint connections triggered the buckling of the pentagon group or hexagon group without resulting in any damage to other joint parts of the dome. The deformation aspect of TPD was investigated by a newly developed numerical program. Simulated results corresponded well with the experimental results under similar loading conditions. Therefore, the hybrid truss method was proved to be an effective method to simulate the TPD structure.

References

1. Faherty KF, Williamson TG (1995) Wood engineering and construction handbook, 2nd edn. McGraw-Hill, New York, pp 9.44–9.50
2. Geers MGD (1999) Enhanced solution control for physically and geometrically non-linear problems, part II. Comparative performance analysis. Int J Numer Meth Eng 46:205–230
3. Worldflower Garden Domes (2004) Type garden dome3. Catalog of Worldflower Garden Domes. Worldflower Garden Domes, Georgetown, TX
4. Meguro K, Tagel-Din H (1997) A new efficient technique for fracture analysis of structures. Bull ERS 30:103–116
5. Yang YQ (1992) Application of structure analysis by finite element method (in Chinese). Dalian Maritime University Press, Dalian, pp 70–72
6. Fuller BR, Applewhite EJ (1975) Synergetics: explorations in the geometry of thinking. MacMillan, New York, pp 1–876